ACS OMEGA

Open Access

http://pubs.acs.org/journal/acsodf

Article

Data-Driven Approaches to Predict Dendrimer Cytotoxicity

Tarun Maity, Anandu K. Balachandran, Lakshmi Priya Krishnamurthy, Karthik L. Nagar, Raghavender S. Upadhyayula,* Shubhashis Sengupta, and Prabal K. Maiti*

Cite This: *ACS Omega* 2024, 9, 24899−24906

Read Online

ACCESS | Metrics & More | Article Recommendations | Supporting Information

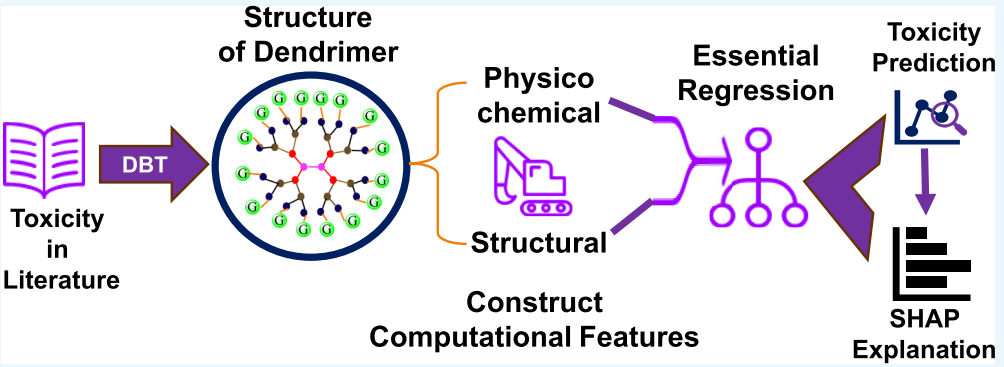

ABSTRACT: Dendrimers are employed as functional elements in contrast agents and are proposed as nontoxic vehicles for drug delivery. Toxicity is a property that is to be evaluated for this novel class of bionanomaterials for in vivo applications. The current research is hampered due to the lack of structured data sets for toxicity studies for dendrimers. In this work, we have built a data set by curating literature for toxicity data and augmented it with structural and physicochemical features. We present a comprehensive, feature-rich database of dendrimer toxicity measured across various cell lines for prediction, design, and optimization studies. We have also explored novel computational approaches for predicting dendrimer cytotoxicity. We demonstrate superior outcomes for toxicity prediction using essential regression in the space of small data sets.

INTRODUCTION

Dendrimers are a class of hyperbranched polymeric molecules with definite three-dimensional structures and tunable architectures.[1] They are characterized by the composition of core, repeating unit, and surface/terminal groups.[2−4] A wide variety of topologies emanating from the different monomers and having an impact on the properties of the dendrimers, for example, size, shape, volume, flexibility, and other physicochemical properties, are reported in the literature.[5−7] Dendrimers provide a robust platform for a range of applications in energy storage,[8] environmental remediation,[9] and biomedicine, particularly as targeted drug delivery vehicles in critical disease treatments.[10−16] Dendrimers are often classified based on the type of branch cell as symmetric (Tomalia-type)[5,6,12] or asymmetric (Denkewalter-type).[17] PAMAM dendrimers are examples of symmetric branched cell dendrimers, and polypeptide/protein-type dendrimers belong to asymmetric branched cell dendrimers. Asymmetric branched cell dendrimers have been exclusively used in a wide range of life sciences applications including antivirals, microbicides, and targeted cancer therapies.[18,19]

Dendrimers, being nanoparticles, are well positioned to be synthesized in a reproducible way with precise control of properties and tunable structural parameters, such as size and surface chemistry, for both therapeutic and diagnostic applications. They have been mostly applied as nanocarriers for biologically active agents. Notably, only dendrimeric nanomedicine is suitable for a wide variety of routes of drug administration, from intravenous to intranasal and transdermal to ocular, and can be used for active or passive drug targeting. Properties such as pharmacokinetics, pharmacodynamics, controlled biodistribution, and toxicity play an important role in the success of dendrimer design. A large number of pharmaceutical companies are investigating the role of lipid nanoparticles, adeno-associated viral vectors, and dendrimers as promising targeted drug delivery routes.

All of these facets of dendrimers render them ideal candidates for nanomedical applications. As compounds that have been intensively studied for their potential role in biomedicine, dendrimers should meet several criteria. Specifically, they should be nontoxic, nonimmunogenic, and

Received: February 23, 2024
Revised: May 10, 2024
Accepted: May 17, 2024
Published: May 27, 2024

biopermeable (to possess the ability to cross bio-barriers), be able to stay in blood circulation until the desired effects occur, and be able to target specific biological molecules. Recently, Banerjee et al. demonstrated the q-RASAR approach for small data set toxicity prediction; this study explores an alternative method using similarity- and error-based descriptors specifically tailored for predicting toxicity in data sets with small, structurally similar molecules.[20−22] Many groups of dendrimers fulfill most of these requirements; however, their utilization in biomedicine is often limited due to their high cytotoxicity.[3,23−29] Predicting the toxicities of compounds is a crucial step in the creation of new drugs.

In this work, we develop data-driven computational approaches to predict the cytotoxicity of dendrimers used in drug delivery. A single database (dendPoint) catering to the study of pharmacokinetic properties of dendrimers has been reported to be of use in the in silico studies.[30] Recently, the advent of predictive modeling using neural networks (artificial intelligence) and recently generative AI (Gen AI) has prompted us to explore the application of these technologies in the space of dendrimer research. In this paper, we present a new data set for studying the cytotoxicity of dendrimers used in drug delivery vehicles in different cell lines.[25] We have manually curated the data set and built initial and optimized 3D structures of the family of the dendrimers reported in the database. We employed in silico techniques to compute and generate features (2D and 3D) characterizing the dendrimers. A battery of recent algorithmic advancements in small data set scenarios for predictive modeling has been employed on the curated data set for dendrimer cytotoxicity prediction, which is prone to the overfitting problem (*curse of dimensionality*).

METHODS

A data-driven machine learning approach to predict cytotoxicity of polymer from structural data is depicted (Figure 1). The workflow involves building three-dimensional (3D) structures of the dendrimers, extracting features from the structures using Mordred to generate additional physicochemical features, and finally utilizing a machine learning model to estimate the cytotoxicity of a given dendrimer.

Curation of the Toxicity Data Set. We have employed a list of dendrimers identified and published by Janaszewska et al.[25] for curating the data set. The curated toxicity levels of the dendrimers investigated in this study are compiled in Table 1. A total of 58 dendrimers were collected, and details on the type of dendrimer, the cell line in which the toxicity was measured, and the level of toxicity observed were extracted from the articles. We realized that toxicity values were not standardized, and the data set required augmentation for predictive tasks.

Standardization of the IC_{50} Values. The IC_{50} values reported for the dendrimers were observed in different measuring units (mg/mL or μg/mL). We standardized the reported values to a common measuring unit (μM).

Generation of 3D Models of Dendrimers. As structural features are considered critical in the design of dendrimers with tunable properties, we have built 3D atomistic structures of all the dendrimers in the data set. The structures were built using our in-house dendrimer builder toolkit (DBT) software (Figure 2).[37] A variety of surface functionals [NH_2, −COOH, −OH, lauroyl ($CH_3(CH_2)_{10}CO^-$), maltose ($C_{12}H_{22}O_{11}$), and maltotriose ($C_{18}H_{32}O_{16}$)] and core groups such as ethyl diamine ($C_2H_8N_2$) and DAB ($C_4H_{12}N_2$) were built by hand. For structures with two distinct surface groups, we generated the larger surface group (lauroyl) and subsequently attached the second surface group using *tleap*[38] and Avogadro.[39]

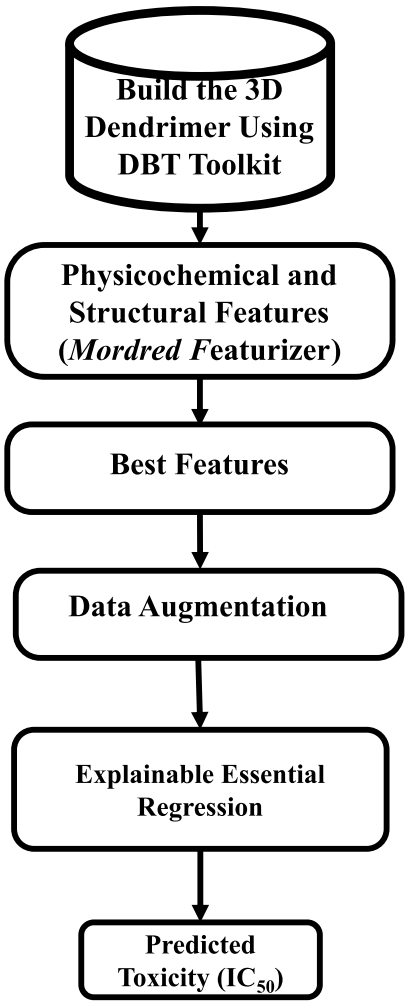

Figure 1. Workflow of data-driven toxicity prediction of dendrimers.

To remove initial unfavorable contacts, each structure was energy minimized for 1000 steps using the steepest descent energy minimization, followed by 1000 steps of conjugate gradient energy minimization using the SANDER tool from AMBER.[38] We used GAFF[40] to describe the intramolecular interactions.

Feature Engineering. The data comprising 58 samples had to be augmented with physicochemical and structural features for studying the patterns for predictive tasks using machine learning. We used Mordred in DeepChem[41] to generate physicochemical features and biological effects[42,43] from the structures. Initial explanatory data analysis involved the following steps:

1. Two sample points, which are above 3× inter quartile range of IC_{50} values, were removed.
2. Structural and physicochemical features were generated using Mordred.
3. The data were augmented via synthetic minority oversampling for regression (SMOTER) by oversampling rare values of a continuous target and selecting k nearest neighbors.[44] This resulted in 137 samples of dendrimers. Gaussian noise was added to these samples to further increase the data set to 276 dendrimers.

https://doi.org/10.1021/acsomega.4c01775
ACS Omega 2024, 9, 24899−24906

Table 1. Summary of the Curated Dendrimer Data Set for Toxicity Prediction

cell line	type	generation	IC_{50} (μM)	ref.
HaCaT	PAMAM	G4 > G5 > G6	16.35 > 1.89 > 1.3	31
B14	PPI	PPI-G4	3.18	32
B16F10	PAMAM	DAB-G2 > G3 > G4	178 > 14.2 > 7.2	
		G 1.5 = G 2.5 = G3.5	155	33
		G1 = G2 > G3 = G4	614 = 614 > 35 = 35	
		DAB G 1.5 = G2.5 = G 3.5	570	
BRL-3A	PPI	PPI-G4	5.93	32
Caco-2	PAMAM	G2 < G2L6 > G2L9	1000 < 15,000 > 1060	
		G2.5 = G3.5 = G2 < G3 > G4	1000 = 1000 = 1000 < 1400 > 130	34
		G4 < G4L3 < G4L6 > G4L9 > G4L15	130 < 360 < 1000 > 100 > 40	
CHO	PAMAM	G3.5 > G4	300 > 46.9	
	PPI	G4 < G4Maltostriose	14.7 < 144.6	35
HaCaT	PAMAM	PPI-G4 > G5 > G6	3.21 > 1.07 > 1.02	31
H4IIE	PAMAM	G3 = G4	500 = 500	36
HepG2	PPI	G4 < G4−100% maltose	6.91 < 100	32
N2a	PPI-G4	G4	3.34	32
SW480	PAMAM	G4 > G5 > G6	23.16 > 5.75 > 3.17	31

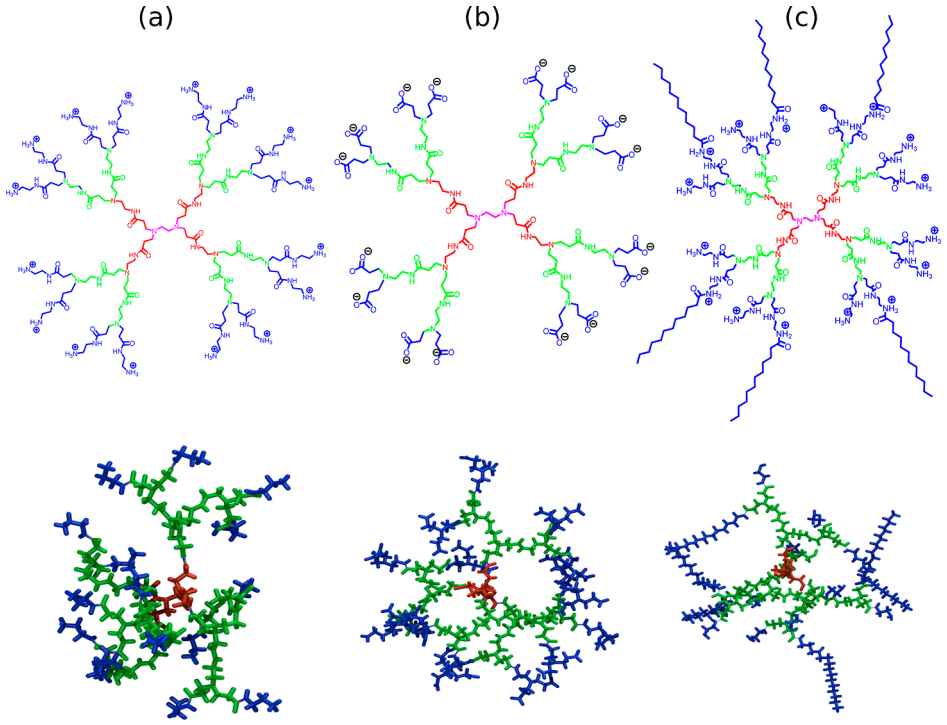

Figure 2. Chemical structure (top row) and energy-minimized structures of dendrimers: (a) G2 PAMAM dendrimer with an EDA core and amino-terminated surface groups, (b) half-generation (G 1.5) PAMAM dendrimer with an EDA core and carboxylic acid-terminated surface groups, and (c) G2 PAMAM dendrimer with two different surface groups: amino and laurel. *Green*: monomeric unit, *blue*: surface unit, and *red*: core.

RESULTS AND DISCUSSION

Predictive Modeling for Dendrimer Toxicity. The data set was subjected to feature reduction using Recursive Feature Elimination in scikit-learn[45] and genetic algorithm in DEAP[46] to reduce the number of features from 1826 to 962 features (see Supporting Information for more details). The data set was split into two buckets of train (n_{train} = 220) and test (n_{test} = 56) samples. With toxicity as a predictive variable, we employed comparative approaches for building machine learning models. Different train/test loading percentage experiments were conducted for selecting the best ratio (80:20) (see Table S1). We addressed the small data problem ($n_{features} \gg n_{samples}$) with data augmentation and an innovative algorithm that allows the building of optimal predictive models. Essential regression (ER) was proposed recently to address the high-dimensionality data sets without any distributional assumptions regarding data. The approach was positioned to identify latent factors and their causal relationships with properties of interest. The approach relies not just on individual observables but on the higher-order relationships encapsulated in the latent factors.[47] We applied ER for dendrimer toxicity prediction, given the high dimensionality of the data set with generated features.

Baseline Regression Approaches. We applied Random Forest as a baseline modeling approach using a few heuristic features to build a predictive model and observed that the

https://doi.org/10.1021/acsomega.4c01775
ACS Omega 2024, 9, 24899−24906

RMSE and MAE were high (Table 2). In molecular embedding-based regression models, molecules are represented as fixed-length numerical vectors, known as embeddings. These embeddings capture essential structural and chemical information about the molecules and are typically derived from the molecular graph, which represents the atoms and their connections within the molecule. The Mol2vec Featurizer was employed to generate embeddings of structural dendrimers. Subsequently, tree-based regression techniques were applied to predict the toxicity.

Table 2. Performance Comparison of Different Modeling Techniques

regression based on	evaluation metrics				
	R^2	RMSE	MAE	Q^2_{F1}	Q^2_{F2}
raw features	0.80	148.68	125.22	0.80	0.80
molecular embedding	0.15	3503.73	1198.67	0.16	0.14
CEF	0.86	127.35	98.56	0.86	0.86
CEP	0.88	114.61	92.74	0.88	0.88
CEF + CEP	0.89	104.58	71.09	0.90	0.89
ER + CEF + CEP	0.92	96.85	43.98	0.93	0.92

Regression Models Based on Crude Estimation of Features and Property. Crude estimation of features (CEF) has been recently shown to enhance model performance in similar small data scenarios in materials sciences.[48] The strategy involves generating crude estimates for features/target properties to address the bias-variance trade-off affecting model precision. We generated crude estimates for features and toxicity (predictive properties) in the feature space and applied regression using random forests (Table 2). Regularization was implemented via hyperparameter fine-tuning and fivefold cross-validation to address and reduce overfitting.

Essential Regression. ER is a regression technique proposed by Bing et al.,[47] which showcases a novel regression technique that identifies causal latent factors responsible for the dependent variable, in our case, dendrimer toxicity. After CEF and crude estimation of property (CEP), we found that the data set perfectly aligned for predictive exploration using the ER framework. We observe that the ER model built with raw features with CEP and CEF performs the best among all approaches (Table 2).

Let us consider the input data as $X \in R^{n*s}$, where s is the sample size and n is the feature size and $Y \in R^s$.

$$X = A*Z + \alpha \tag{1}$$

$$Y = Z^T*\beta + \epsilon \tag{2}$$

The input matrix X is decomposed into allocation matrix A and latent matrix Z, where $A \in R^{n*k}$, $Z \in R^{k*s}$, and $\beta \in R^k$ are regression coefficients, and $\alpha \in R^{n*s}$ and $\epsilon \in R^s$ are irreducible independent error terms.

The allocation matrix is obtained using the principal component analysis technique, by calculating the eigenvectors of the covariance matrix $\Sigma = \frac{1}{(s-1)}*X*X^T$, where the eigenvectors v_i are obtained by solving $\sum v_i = \lambda_i*v_i$; here, λ_i represents the eigenvalues. By selecting the top k eigenvectors, a reduced-dimensional space is formed, which is the allocation matrix $A \in R^{n*k}$. The latent factor matrix Z is then formed by using eq 1. This matrix, which consists of relevant features, is then used for regression to generate the output matrix Y.

Explainable ER for Toxicity Prediction. Model performance metrics for test samples are reported in Table 2. Of all the data-driven approaches for toxicity prediction, ER with crude estimates of features and properties produced superior results with an RMSE of 96.85, MAE of 43.98, and R^2 of 0.92. A plot of predictions against ground truth toxicity IC_{50} values is shown in Figure 3. The model predictions are, in general, in good agreement with ground truth values. We also observe that in a few cases involving PAMAM-G4-L9, PAMAM-G2.5

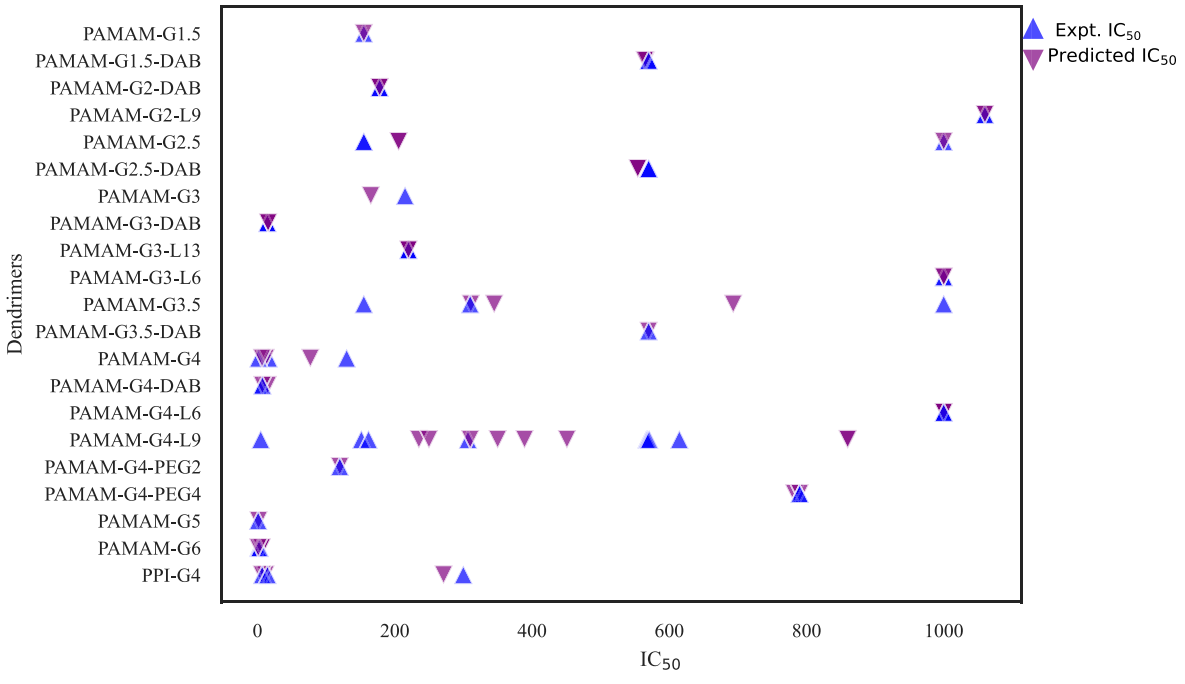

Figure 3. Prediction of IC_{50} values based on ER.

https://doi.org/10.1021/acsomega.4c01775
ACS Omega 2024, 9, 24899−24906

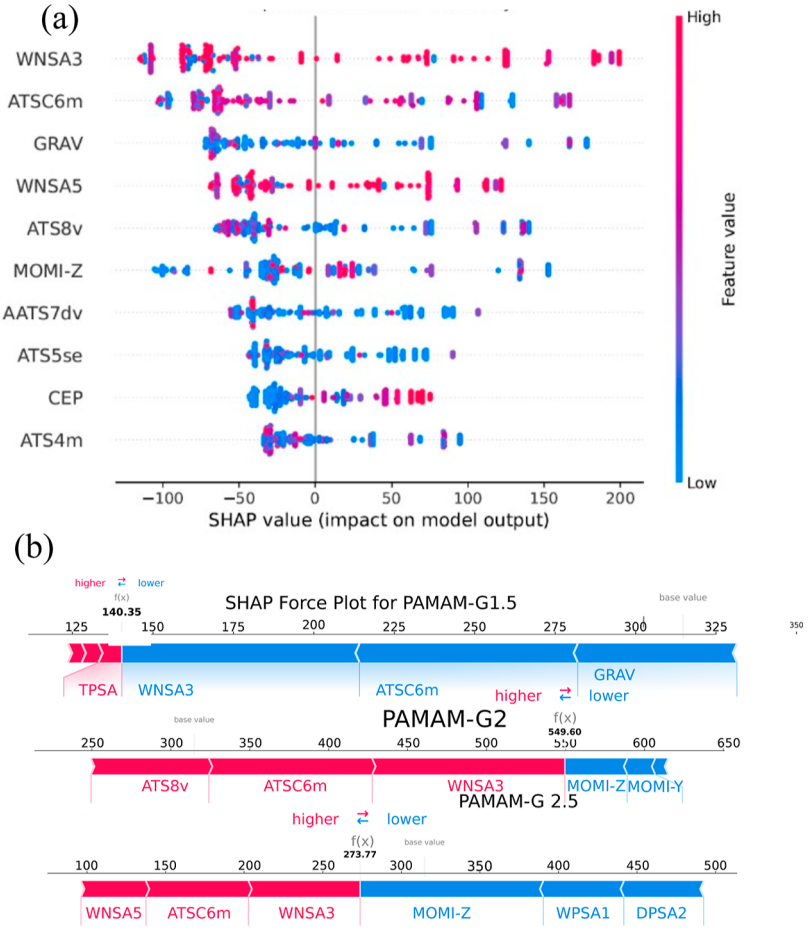

Figure 4. (a) SHAP (SHapley Additive exPlanations) summary plots for key features influencing model predictions of PAMAM dendrimer generations. (b) SHAP force plot for PAMAM (G1.5, G2, and G2.5) to determine which features are more important for particular generations. TPSA dominates for G1.5, while WNSA3/5 (surface-weighted charged area) and ATSC6m (mass distribution within 6 bonds) are most impactful for G2 and G2.5. These features relate to charge, surface area, size, shape, and mass distribution, influencing potential biological activity.

PAMAM-G3.5, and PAMAM-G3, the predictions are off beyond the mean absolute error of 43.98 μM.

SHAP[49,50] summary plot provides insights into features that have the most impact on the model predictions (Figure 4). Among the top 10 SHAP features, surface area descriptors (WNSA3 and WNSA5) and autocorrelation descriptors (ATSC6m, ATS8v, AATS7dv, and ATS5se) emerge as significant and play a crucial role in the toxicity of the polymer (Figure 4). Surface area descriptors, which measure the negatively charged surface area, can change how dendrimers interact with biological molecules or cell membrane,[51] which could make them toxic.[52] Moreau−Broto autocorrelation descriptors like ATSC6m, ATS8v, AATS7dv, ATS5se, and ATS7i capture the distribution of properties like mass, van der Waals volume, valence electrons, Sanderson electronegativity, and ionization potential across the dendrimer structure, influencing its interactions with biological systems and thus its toxicity.[53] The heavy atom gravitational index (GRAV) and the moment of inertia (MOMI-Z) provide insights into the molecular weight and shape of the dendrimer, respectively, both of which can affect how the dendrimer is processed by biological systems or translocated across the biological membrane[54] and its subsequent toxicity.[51,53] Overall, these features representing the size, surface charge density, and mass distribution of dendrimers primarily influence their interaction and the contacts between their surfaces and the constituents of blood and tissues as well as the surfaces of blood vessels. These interactions can lead to potential membrane disruption and cytotoxicity.[55,56] We describe below individual predictions for a few cases pertaining to the dendrimer of generations 1.5, 2, and 2.5 (G1.5, G2, and G2.5) and the explanations for the predictions. SHAP force plots for predictions of test samples from other generations are available in Supporting Information (Figure S3). For PAMAM-G1.5, total polar surface area (TPSA) is seen to contribute positively toward prediction, whereas for both PAMAM-G2 and G2.5, SHAP force plots point to WNSA3 and ATSC6m as common factors for a positive attribution to predicted values. WNSA3, being surface-weighted charged partial negative surface area, has implications for the electrostatic and hydrogen bonding potential of the molecule, and ATSC6m (centered Moreau−Broto autocorrelation of lag 6 weighted by mass) explains the distribution of mass within six bonds in a molecule. SHAP force plots for predictions of test samples from other generations are available in Supporting Information (Figure S3).

CONCLUSIONS

We report a comprehensive feature-rich toxicity data set capturing a variety of physicochemical features of dendrimers in experiments performed in different cell lines. The data set is envisaged to complement the existing data sets for studying the pharmacogenomic impact of these synthetic polymers in

https://doi.org/10.1021/acsomega.4c01775
ACS Omega 2024, 9, 24899−24906

humans.[30] To the best of our knowledge, this is the first report on use of predictive modeling approaches for predicting the cytotoxicity of dendrimers. The exploration of different computational approaches led to a model based on ER, which is seen to perform predictive tasks considerably well. The model performance with ER indicates that minimal and conservative data augmentation approaches can lead to a performant model in low-data scenarios. Handling features in the canonical space for predictive tasks in these scenarios is usually achieved with dimensionality reduction. On the contrary, ER takes a different approach by projecting these features and clustering them in latent space. In addition, the generation of crude estimates of features and target variables also leads to a scientifically explainable, minimalistic data engineering approach. Experiments on a prioritized set of hypotheses, for example, dendrimers as preferred vehicles of choice for drug delivery, will benefit with the design and optimization of nontoxic dendrimers for in vivo experiments via in silico approaches. Compared with traditional in vivo testing with model organisms, computational toxicity estimations offer remarkable advantages, primarily because they are faster than the determination of toxic doses in actual animal or cell line experiments. These computational approaches will help reduce the cost and timescale of in vivo experiments on model organisms. We also describe the application of the algorithms implemented in this report to the design and optimization of antibody−drug conjugates, specifically, the design of linkers. Toxicity prediction approaches can increase the pace of discovery and acceptance of the safe and efficient use of dendrimers as drug conjugates.

■ ASSOCIATED CONTENT

Data Availability Statement

All the dendrimer structures and codes reported in this article have been deposited at Zenodo (https://zenodo.org/records/11044638).

Supporting Information

The Supporting Information is available free of charge at https://pubs.acs.org/doi/10.1021/acsomega.4c01775.

IC_{50} distribution and variation across cell lines; model interpretability with SHAP force plots; essential regression performance across training set variations; and top 10 most influential features identified for cytotoxicity prediction (PDF)

■ AUTHOR INFORMATION

Corresponding Authors

Raghavender S. Upadhyayula − *Accenture Labs, Technology & Innovation, Bengaluru 560087, India*; Email: r.surya.upadhyayula@accenture.com

Prabal K. Maiti − *Centre for Condensed Matter Theory, Department of Physics, Indian Institute of Science, Bengaluru 560012, India*; orcid.org/0000-0002-9956-1136; Email: maiti@iisc.ac.in

Authors

Tarun Maity − *Centre for Condensed Matter Theory, Department of Physics, Indian Institute of Science, Bengaluru 560012, India*; orcid.org/0000-0002-4405-0371

Anandu K. Balachandran − *Accenture Labs, Technology & Innovation, Bengaluru 560087, India*; orcid.org/0000-0003-0068-8047

Lakshmi Priya Krishnamurthy − *Accenture Labs, Technology & Innovation, Bengaluru 560087, India*

Karthik L. Nagar − *Accenture Labs, Technology & Innovation, Bengaluru 560087, India*

Shubhashis Sengupta − *Accenture Labs, Technology & Innovation, Bengaluru 560087, India*

Complete contact information is available at: https://pubs.acs.org/10.1021/acsomega.4c01775

Notes

The authors declare no competing financial interest.

■ ACKNOWLEDGMENTS

T.M. thanks Accenture for the internship opportunity and also the Ministry of Education (MOE), India, for the fellowship.

■ REFERENCES

(1) Pramanik, D.; Kanchi, S.; Ayappa, K. G.; Maiti, P. K.. In *Computational Materials, Chemistry, and Biochemistry: From Bold Initiatives to the Last Mile: In Honor of William A. Goddard's Contributions to Science and Engineering*; Shankar, S., Muller, R., Dunning, T., Chen, G. H., Eds.; Springer International Publishing: Cham, 2021; pp 411−449.

(2) Helms, B.; Meijer, E. Dendrimers at work. *Science* **2006**, *313*, 929−930.

(3) Svenson, S.; Tomalia, D. A. Dendrimers in biomedical applications—reflections on the field. *Adv. Drug Deliv. Rev.* **2012**, *64*, 102−115.

(4) Maiti, P. K.; Çağın, T.; Wang, G.; Goddard, W. A. Structure of PAMAM dendrimers: generations 1 through 11. *Macromolecules* **2004**, *37*, 6236−6254.

(5) Tomalia, D. A.; Baker, H.; Dewald, J.; Hall, M.; Kallos, G.; Martin, S.; Roeck, J.; Ryder, J.; Smith, P. A new class of polymers: starburst-dendritic macromolecules. *Polym. J.* **1985**, *17*, 117−132.

(6) Tomalia, D. A.; Naylor, A. M.; Goddard, W. A., III Starburst dendrimers: molecular-level control of size, shape, surface chemistry, topology, and flexibility from atoms to macroscopic matter. *Angew Chem. Int. Ed. Engl.* **1990**, *29*, 138−175.

(7) Maiti, P. K.; Çağın, T.; Lin, S.-T.; Goddard, W. A. Effect of solvent and pH on the structure of PAMAM dendrimers. *Macromolecules* **2005**, *38*, 979−991.

(8) Maity, T.; Gosika, M.; Pascal, T. A.; Maiti, P. K. Molecular insights into the physics of poly (amidoamine)-dendrimer-based supercapacitors. *Phys. Rev. Appl.* **2022**, *18*, 054031.

(9) Maity, T.; Aggarwal, A.; Dasgupta, S.; Velachi, V.; Singha Deb, A. K.; Ali, S. M.; Maiti, P. K. Efficient removal of uranyl ions using PAMAM dendrimer: simulation and experiment. *Langmuir* **2023**, *39*, 6794−6802.

(10) Pandita, D.; Madaan, K.; Kumar, S.; Poonia, N.; Lather, V. Dendrimers in drug delivery and targeting: drug-dendrimer interactions and toxicity issues. *J. Pharm. BioAllied Sci.* **2014**, *6*, 139.

(11) Maingi, V.; Kumar, M. V. S.; Maiti, P. K. PAMAM dendrimer−drug interactions: effect of pH on the binding and release pattern. *J. Phys. Chem. B* **2012**, *116*, 4370−4376.

(12) Vasumathi, V.; Maiti, P. K. Complexation of siRNA with dendrimer: a molecular modeling approach. *Macromolecules* **2010**, *43*, 8264−8274.

(13) Nandy, B.; Maiti, P. K. DNA compaction by a dendrimer. *J. Phys. Chem. B* **2011**, *115*, 217−230.

(14) Lakshminarayanan, A.; Ravi, V. K.; Tatineni, R.; Rajesh, Y. B. R. D.; Maingi, V.; Vasu, K. S.; Madhusudhan, N.; Maiti, P. K.; Sood, A. K.; Das, S.; et al. Efficient dendrimer−DNA complexation and gene delivery vector properties of nitrogen-core poly (propyl ether imine) dendrimer in mammalian cells. *Bioconjugate Chem.* **2013**, *24*, 1612−1623.

(15) Maiti, P. K.; Bagchi, B. Structure and dynamics of DNA-dendrimer complexation: role of counterions, water, and base pair sequence. *Nano Lett.* **2006**, *6*, 2478−2485.
(16) Sherje, A. P.; Jadhav, M.; Dravyakar, B. R.; Kadam, D. Dendrimers: a versatile nanocarrier for drug delivery and targeting. *Int. J. Pharm.* **2018**, *548*, 707−720.
(17) Denkewalter, R. G.; Kolc, J.; Lukasavage, W. J. Macromolecular highly branched homogeneous compound based on lysine units. U.S. Patent 4,289,872 A, 1981.
(18) Nandy, B.; Bindu, D. H.; Dixit, N. M.; Maiti, P. K. Simulations reveal that the HIV-1 gp120-CD4 complex dissociates via complex pathways and is a potential target of the polyamidoamine (PAMAM) dendrimer. *J. Chem. Phys.* **2013**, *139*, 024905.
(19) Nandy, B.; Saurabh, S.; Sahoo, A. K.; Dixit, N. M.; Maiti, P. K. The SPL7013 dendrimer destabilizes the HIV-1 gp120−CD4 complex. *Nanoscale* **2015**, *7*, 18628−18641.
(20) Chatterjee, M.; Banerjee, A.; De, P.; Gajewicz-Skretna, A.; Roy, K. A novel quantitative read-across tool designed purposefully to fill the existing gaps in nanosafety data. *Environ. Sci.: Nano* **2022**, *9*, 189−203.
(21) Banerjee, A.; Roy, K. First report of q-RASAR modeling toward an approach of easy interpretability and efficient transferability. *Mol. Diversity* **2022**, *26*, 2847−2862.
(22) Banerjee, A.; Chatterjee, M.; De, P.; Roy, K. Quantitative predictions from chemical read-across and their confidence measures. *Chemom. Intell. Lab. Syst.* **2022**, *227*, 104613.
(23) Esfand, R.; Tomalia, D. A. Poly (amidoamine)(PAMAM) dendrimers: from biomimicry to drug delivery and biomedical applications. *Drug Discov. Today* **2001**, *6*, 427−436.
(24) Jain, K.; Kesharwani, P.; Gupta, U.; Jain, N. Dendrimer toxicity: let's meet the challenge. *Int. J. Pharm.* **2010**, *394*, 122−142.
(25) Janaszewska, A.; Lazniewska, J.; Trzepinski, P.; Marcinkowska, M.; Klajnert-Maculewicz, B. Cytotoxicity of dendrimers. *Biomolecules* **2019**, *9*, 330.
(26) Gupta, U.; Dwivedi, S. K. D.; Bid, H. K.; Konwar, R.; Jain, N. Ligand anchored dendrimers based nanoconstructs for effective targeting to cancer cells. *Int. J. Pharm.* **2010**, *393*, 186−197.
(27) Agashe, H. B.; Dutta, T.; Garg, M.; Jain, N. Investigations on the toxicological profile of functionalized fifth-generation poly (propylene imine) dendrimer. *J. Pharm. Pharmacol.* **2010**, *58*, 1491−1498.
(28) Patel, S. K.; Gajbhiye, V.; Jain, N. K. Synthesis, characterization and brain targeting potential of paclitaxel loaded thiamine-PPI nanoconjugates. *J. Drug Targeting* **2012**, *20*, 841−849.
(29) Balogh, L.; Swanson, D. R.; Tomalia, D. A.; Hagnauer, G. L.; McManus, A. T. Dendrimer-silver complexes and nanocomposites as antimicrobial agents. *Nano Lett.* **2001**, *1*, 18−21.
(30) Kaminskas, L. M.; Pires, D. E.; Ascher, D. B. dendPoint: a web resource for dendrimer pharmacokinetics investigation and prediction. *Sci. Rep.* **2019**, *9*, 15465.
(31) Mukherjee, S. P.; Lyng, F. M.; Garcia, A.; Davoren, M.; Byrne, H. J. Mechanistic studies of in vitro cytotoxicity of poly (amidoamine) dendrimers in mammalian cells. *Toxicol. Appl. Pharmacol.* **2010**, *248*, 259−268.
(32) Felczak, A.; Wrońska, N.; Janaszewska, A.; Klajnert, B.; Bryszewska, M.; Appelhans, D.; Voit, B.; Różalska, S.; Lisowska, K. Antimicrobial activity of poly (propylene imine) dendrimers. *New J. Chem.* **2012**, *36*, 2215−2222.
(33) Malik, N.; Wiwattanapatapee, R.; Klopsch, R.; Lorenz, K.; Frey, H.; Weener, J.; Meijer, E.; Paulus, W.; Duncan, R. Dendrimers::relationship between structure and biocompatibility in vitro, and preliminary studies on the biodistribution of 125I-labelled polyamidoamine dendrimers in vivo. *J. Controlled Release* **2000**, *65*, 133−148.
(34) Jevprasesphant, R.; Penny, J.; Attwood, D.; McKeown, N. B.; D'Emanuele, A. Engineering of dendrimer surfaces to enhance transepithelial transport and reduce cytotoxicity. *Pharm. Res.* **2003**, *20*, 1543−1550.
(35) Janaszewska, A.; Maczynska, K.; Matuszko, G.; Appelhans, D.; Voit, B.; Klajnert, B.; Bryszewska, M. Cytotoxicity of PAMAM, PPI and maltose modified PPI dendrimers in Chinese hamster ovary (CHO) and human ovarian carcinoma (SKOV3) cells. *New J. Chem.* **2012**, *36*, 428−437.
(36) Hernando, M.; Rosenkranz, P.; Ulaszewska, M.; Fernández-Cruz, M. L.; Fernández-Alba, A. R.; Navas, J. In vitro dose−response effects of poly (amidoamine) dendrimers [amino-terminated and surface-modified with N-(2-hydroxydodecyl) groups] and quantitative determination by a liquid chromatography−hybrid quadrupole/time-of-flight mass spectrometry based method. *Anal. Bioanal. Chem.* **2012**, *404*, 2749−2763.
(37) Maingi, V.; Jain, V.; Bharatam, P. V.; Maiti, P. K. Dendrimer building toolkit: model building and characterization of various dendrimer architectures. *J. Comput. Chem.* **2012**, *33*, 1997−2011.
(38) Cornell, W. D.; Cieplak, P.; Bayly, C. I.; Gould, I. R.; Merz, K. M.; Ferguson, D. M.; Spellmeyer, D. C.; Fox, T.; Caldwell, J. W.; Kollman, P. A. A second generation force field for the simulation of proteins, nucleic acids, and organic molecules. *J. Am. Chem. Soc.* **1995**, *117*, 5179−5197.
(39) Hanwell, M. D.; Curtis, D. E.; Lonie, D. C.; Vandermeersch, T.; Zurek, E.; Hutchison, G. R. Avogadro: an advanced semantic chemical editor, visualization, and analysis platform. *J. Cheminf.* **2012**, *4*, 17.
(40) Wang, J.; Wolf, R. M.; Caldwell, J. W.; Kollman, P. A.; Case, D. A. Development and testing of a general amber force field. *J. Comput. Chem.* **2004**, *25*, 1157−1174.
(41) Ramsundar, B.; Eastman, P.; Walters, P.; Pande, V.; Leswing, K.; Wu, Z. *Deep Learning for the Life Sciences*; O'Reilly Media, 2019.
(42) Ferraz-Caetano, J.; Teixeira, F.; Cordeiro, M. N. D. Explainable supervised machine learning model to predict solvation Gibbs energy. *J. Chem. Inf. Model.* **2023**, *64*, 2250−2262.
(43) Zaslavskiy, M.; Jégou, S.; Tramel, E. W.; Wainrib, G. ToxicBlend: virtual screening of toxic compounds with ensemble predictors. *Comput. Toxicol.* **2019**, *10*, 81−88.
(44) Torgo, L.; Ribeiro, R.; Pfahringer, B.; Branco, P. SMOTE for regression. *Progress in Artificial Intelligence*; Springer, 2013; pp 378−389.
(45) Pedregosa, F.; et al. Scikit-learn: machine learning in Python. *J. Mach. Learn. Res.* **2011**, *12*, 2825−2830.
(46) Fortin, F.-A.; De Rainville, F.-M.; Gardner, M.-A.; Parizeau, M.; Gagné, C. DEAP: evolutionary algorithms made easy. *J. Mach. Learn. Res.* **2012**, *13*, 2171−2175.
(47) Bing, X.; Lovelace, T.; Bunea, F.; Wegkamp, M.; Kasturi, S. P.; Singh, H.; Benos, P. V.; Das, J. Essential regression: a generalizable framework for inferring causal latent factors from multi-omic datasets. *Patterns* **2022**, *3*, 100473.
(48) Zhang, Y.; Ling, C. A strategy to apply machine learning to small datasets in materials science. *npj Comput. Mater.* **2018**, *4*, 25.
(49) Lundberg, S. M.; Nair, B.; Vavilala, M. S.; Horibe, M.; Eisses, M. J.; Adams, T.; Liston, D. E.; Low, D. K. W.; Newman, S. F.; Kim, J.; et al. Explainable machine-learning predictions for the prevention of hypoxaemia during surgery. *Nat. Biomed. Eng.* **2018**, *2*, 749−760.
(50) Lundberg, S. M.; Lee, S.-I. A unified approach to interpreting model predictions. In *Advances in Neural Information Processing Systems*, 2017.
(51) Bhattacharya, R.; Kanchi, S.; Roobala, C.; Lakshminarayanan, A.; Seeck, O. H.; Maiti, P. K.; Ayappa, K. G.; Jayaraman, N.; Basu, J. K. A new microscopic insight into membrane penetration and reorganization by PETIM dendrimers. *Soft Matter* **2014**, *10*, 7577−7587.
(52) Tomalia, D. A.; Christensen, J. B.; Boas, U. *Dendrimers, Dendrons, and Dendritic Polymers: Discovery, Applications, and the Future*; Cambridge University Press, 2012.
(53) Kannan, R.; Nance, E.; Kannan, S.; Tomalia, D. A. Emerging concepts in dendrimer-based nanomedicine: from design principles to clinical applications. *J. Intern. Med.* **2014**, *276*, 579−617.
(54) Sahoo, A. K.; Kanchi, S.; Mandal, T.; Dasgupta, C.; Maiti, P. K. Translocation of bioactive molecules through carbon nanotubes embedded in the lipid membrane. *ACS Appl. Mater. Interfaces* **2018**, *10*, 6168−6179.

https://doi.org/10.1021/acsomega.4c01775
ACS Omega 2024, 9, 24899−24906

(55) Nel, A.; Xia, T.; Meng, H.; Wang, X.; Lin, S.; Ji, Z.; Zhang, H. Nanomaterial toxicity testing in the 21st century: use of a predictive toxicological approach and high-throughput screening. *Acc. Chem. Res.* **2013**, *46*, 607−621.
(56) Luan, F.; Kleandrova, V. V.; González-Díaz, H.; Ruso, J. M.; Melo, A.; Speck-Planche, A.; Cordeiro, M. N. D. S. Computer-aided nanotoxicology: assessing cytotoxicity of nanoparticles under diverse experimental conditions by using a novel QSTR-perturbation approach. *Nanoscale* **2014**, *6*, 10623−10630.

https://doi.org/10.1021/acsomega.4c01775
ACS Omega 2024, 9, 24899−24906